

## PREDICTIONS OF THE TIME COURSE OF FORCE AND POWER OUTPUT BY DOGFISH WHITE MUSCLE FIBRES DURING BRIEF TETANI

N. A. CURTIN<sup>1,\*</sup>, A. R. GARDNER-MEDWIN<sup>2</sup> AND R. C. WOLEDGE<sup>2,3</sup>

<sup>1</sup>*Department of Physiology, Charing Cross and Westminster Medical School, Fulham Palace Road, London W6 8RF, UK,* <sup>2</sup>*Department of Physiology, University College London, Gower Street, London WC1E 6BT, UK* and <sup>3</sup>*Institute of Human Performance, University College London, Royal National Orthopaedic Hospital Trust, Brockley Hill, Stanmore, Middlesex HA7 4LP, UK*

\*e-mail: n.curtin@cxwms.ac.uk

Accepted 13 October 1997

### Summary

The aim of this study was to identify the principal factors that determine the time course of force and power output by muscle during patterns of stimulation and movement similar to those during fish swimming. Fully activated, white muscle fibres isolated from dogfish *Scyliorhinus canicula* were used to characterize the force–velocity relationship of the contractile component (CC) and the stress–strain relationship of the passive, elastic component (SEC) in series with the CC. A simple model of the time course of crossbridge activation during brief contractions was devised. Using the mechanical properties of the CC and SEC and the activation time course, force and power were predicted for brief contractions with constant-velocity movement and also for brief contractions starting at various times during sinusoidal movement. The predicted force and power were compared with observations for

these patterns of stimulation and movement. The predictions matched the observations well for the period during stimulation. Matching of force was much less good for some specific conditions during relaxation, the period during which force persists after the end of stimulation. If either the slow rise of activation or the SEC was omitted from the calculation, the predictions were poor, even during stimulation. Additional factors which may influence force are discussed. These include the after-effects of shortening and stretch, the variation of force during constant-velocity stretch and non-uniform behaviour within the muscle.

Key words: muscle contraction, series elasticity, series compliance, force–velocity relationship, power, white muscle fibre, dogfish, *Scyliorhinus canicula*, fish muscle.

### Introduction

The work described here investigates the extent to which the time course of active force and power during contractions can be explained on the basis of a set of simple principles. Contractions with constant-velocity shortening and lengthening, as well as sinusoidal movements, are considered. Our approach extends the work of Hill (1938, 1970) and Jewell and Wilkie (1958) in that we consider brief tetani in which much of the movement occurs while force is developing. Also, we include tetani during sinusoidal in addition to constant-velocity movement. Thus, we consider contractions similar to those occurring during muscle function *in vivo*.

The major determinants of the speed of filament sliding are expected to be (a) the external force opposing the sliding movement, and (b) the extent to which the population of crossbridges is active, by which we mean capable of cycles of interaction with actin. Therefore, the time course over which force is developed and then decays during a cycle of stimulation and relaxation is expected to be determined primarily by (1) the time course over which crossbridge activation rises and falls, (2) the relationships between force,

crossbridge activation, direction and speed of filament sliding, and (3) the compliance of the series elastic component.

The force exerted during contraction is profoundly influenced by the extent and speed of filament sliding. It has long been recognised, but is not always appreciated, that significant sliding occurs even in contractions during which the muscle's ends are kept fixed in position. The sliding occurs in these nominally isometric contractions because the force developed by the crossbridges is transmitted to the restraints at the muscle ends through structures that are compliant. This compliance is partly in the tendons and aponeuroses (internal tendinous sheets) and partly in the myofilaments. We will use the term series elastic component (SEC) for these compliances. The elasticity in the crossbridges themselves is not part of the SEC in this sense, because its existence does not lead to filament sliding as force develops. Also, the crossbridges are very stiff compared with structures in series with them. The crossbridge stiffness measured by Ford *et al.* (1977) is approximately 13 times greater than the highest value measured here for the SEC.

In this study, our strategy is to (1) measure the stiffness of the SEC and the standard relationship between force and constant-velocity filament sliding when the muscle is fully activated, (2) to observe the force–velocity relationship for brief tetani during both ramp and sinusoidal length changes, when activation, filament sliding and strain in the SEC are not constant, (3) to evaluate the effect of the SEC on movement, and (4) to determine how well the time course of force and power can be predicted by taking account of both the measured mechanical properties of the SEC and fully active muscle and of a simple model of the time course of crossbridge activation during brief contractions.

Many factors known to influence force development are not included in our simple model. For example, the model does not take account of the after-effects of either shortening (Edman, 1975; Edman *et al.* 1993) or stretch (Lombardi and Piazzesi, 1990; Edman and Tsuchiya, 1996), nor the consequences of non-uniform length changes, particularly during relaxation (Curtin and Edman, 1989). The intention is not, of course, to suggest a denial that these effects exist but to determine, first, how important are the consequences of series elasticity and varying activation in *in-vivo*-like contractions and, second, what discrepancies exist between the data and our simple predictions, which may require these other effects to be taken into account.

Related work has been carried out on lamprey muscle (Williams *et al.* 1997).

## Materials and methods

### *Experiments on isolated muscle*

Dogfish *Scyliorhinus canicula* (L.) were killed by decapitation followed by pithing. Bundles of fibres were dissected under saline from thin slices of the white myotomal muscle taken from the immediate post-anal region. A piece of myoseptum at each end of the bundle was held in an aluminium foil clip. The saline solution contained (in mmol l<sup>-1</sup>): NaCl, 292.0; KCl, 3.2; CaCl<sub>2</sub>, 5.0; MgSO<sub>4</sub>, 1.0; Na<sub>2</sub>SO<sub>4</sub>, 1.6; NaHCO<sub>3</sub>, 5.9; urea, 483; tubocurarine, 1.5 mg l<sup>-1</sup>. The composition is based on the standard Plymouth elasmobranch saline.

The experiments were carried out at 12 °C with the fibre bundle mounted horizontally between a semi-conductor strain gauge force transducer and a combined motor and length transducer (Cambridge Technology, Inc., series 300B lever system). The preparation was electrically stimulated with constant current pulses (Digitimer Stimulator, model DS7). Stimulus frequency was adjusted to give a fused tetanus and was 34.5 Hz. In each experiment, the relationship between stimulus strength and isometric force was investigated to establish supramaximal stimulus strength.

The relationship between fibre length and force was also investigated so that appropriate initial and final lengths, on the plateau of the length–tension relationship, could be chosen for the experiments using tetani with movement. In fact, the isometric force at the long, middle and short lengths varied by less than 2%.  $L_0$  was defined as the fibre length at which force in an isometric tetanus is greatest.

Digitimers and a commercial oscillator provided the control signals for the stimulator and motor. Force and motor position were recorded on a digital oscilloscope and transferred to a PC using WaveForm Basic software.

Three types of experiment were performed on the muscle preparation.

### *Experiment 1*

The series elasticity and the force–velocity relationship during full crossbridge activation were characterized. In the following, motor velocity and movement are designated with the subscript E to distinguish them from velocity and movement of filament sliding within the contractile component, which is designated by the subscript CC. Movement<sub>E</sub> started after 192 ms of stimulation under isometric conditions. For shortening, the pattern of movement<sub>E</sub> was a step followed by constant-velocity (ramp) movement<sub>E</sub> with continuing stimulation, as shown in Fig. 1A. Different step sizes were tried with each ramp velocity to find the step size that reduced the force to match the level that could be produced during subsequent shortening. When step size was too small, force continued to decrease during the ramp shortening, whereas when it was too large, force increased. Steps of the appropriate size gave force records such as those shown in Fig. 1A. For stretches, constant-velocity movement was used. Force increases continuously during stretching at the relatively low velocities ( $V$ ) used here. The force and  $V_{CC}$  values shown in Fig. 1D are the mean values during a stretch of 0.75 mm, as in experiments 2 and 3 described below.  $V_{CC}$  is derived from  $V_E$  and the stiffness of the SEC, which is assumed to be constant at 21 dimensionless units (see Results).

### *Experiment 2*

Force during ramp movement<sub>E</sub> with incomplete crossbridge activity was investigated. Movement<sub>E</sub> started 40 ms before stimulation. Each tetanus consisted of 10 stimuli at 34.5 Hz (stimulus burst 290 ms). The distance moved was 0.75 mm, which was equivalent to 12.5%  $L_0$  (see Fig. 2A).

### *Experiment 3*

Force during sinusoidal movement<sub>E</sub> with 290 ms tetanic stimulation was investigated. The peak-to-peak distance moved (0.75 mm) and the frequency and duration of stimulation were as in the ramp movements<sub>E</sub> in experiment 2 described above. The sinusoidal movement<sub>E</sub> occurred at 1.25 Hz (cycle time 800 ms) and was centred around  $L_0$ . Stimulus phase designates the timing of the stimulus relative to the movement<sub>E</sub> and is defined as the time from the beginning of muscle stimulation to the beginning of shortening expressed as a percentage of the duration of the movement<sub>E</sub> cycle. Stimulus phases of 0% (Fig. 2Bi), 20% (Fig. 2Bii), 40% (Fig. 2Biii), 60% (Fig. 2Biv) and 80% (Fig. 2Bv) were tested.

Similar results were obtained in experiments on three muscle fibre preparations from different fish. One set of results are presented here in detail.

### *Predictions of force and power*

The predictions of force production during 290 ms of tetanic

stimulation with ramp or sinusoidal movement<sub>E</sub> as described in experiments 2 and 3 above were calculated by numerical integration using the stimulus duration and movement<sub>E</sub> pattern shown in Fig. 2 and the relationships shown in Figs 1C, 5 and 6. Power was calculated as the product of force (observed or predicted) and velocity of motor movement ( $V_E$ ) at the corresponding time.

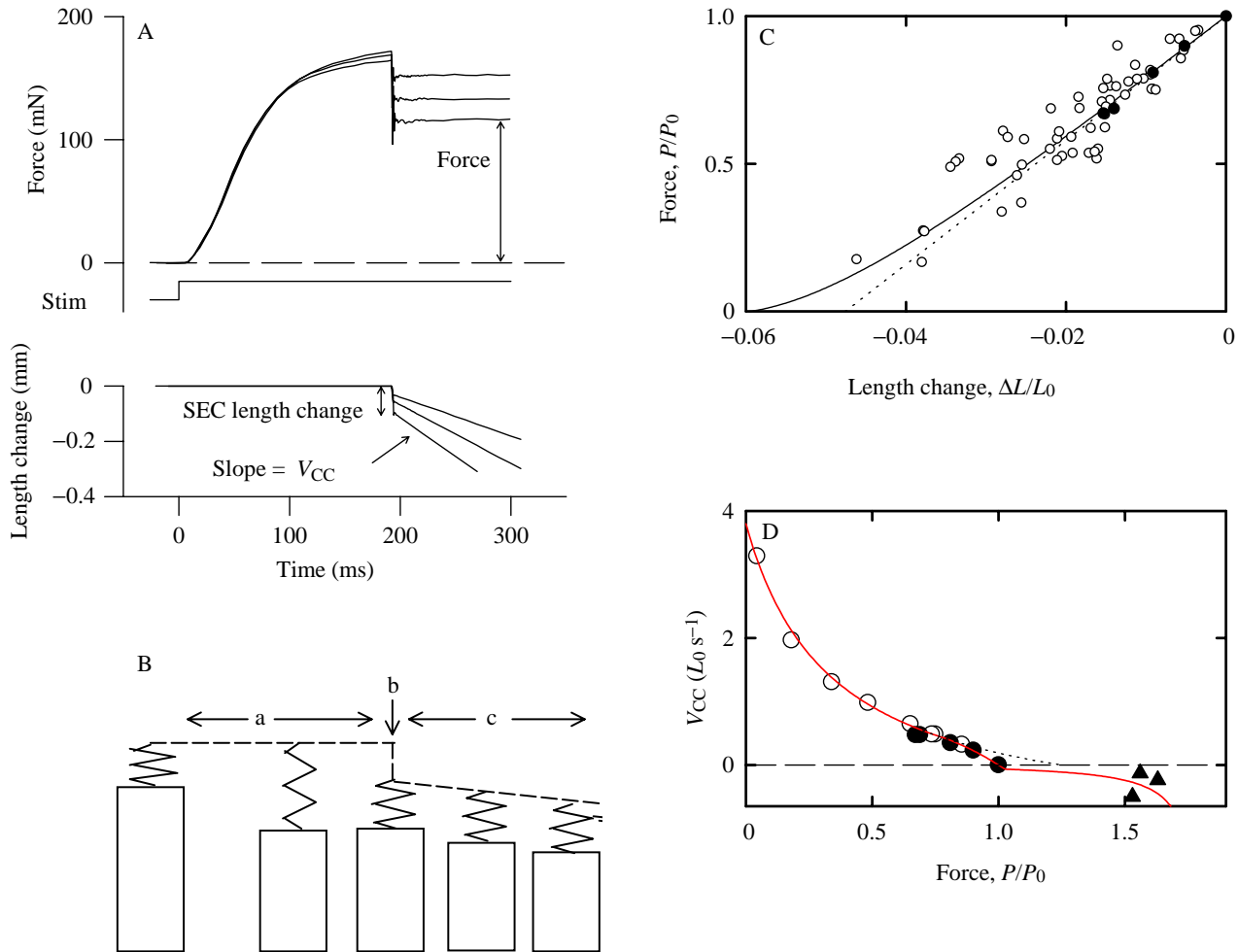


Fig. 1. (A) Three superimposed records of force and length change during tetanic stimulation. Arrows indicate where measurements were made for plotting in C and D.  $V_{CC}$ , velocity of filament sliding within the contractile component. SEC, series elastic component. (B) Diagram illustrating the lengths of the contractile component (block) and series elastic component (zig-zag line) at rest, just before the step change in length (a), at the end of the step (b) and during constant-velocity (ramp) shortening (c). The time scale is the same as in A. (C) Stress-strain relationship for the series elastic component. The force at the end of the step ( $P$ ) expressed relative to the force before the step ( $P_0$ ) is used as a measure of stress. The length change during the step ( $\Delta L$ ) expressed relative to the muscle length giving maximum isometric force ( $L_0$ ) is taken as a measure of strain. The dotted line is the best-fit straight line through the filled circles, which are from the same muscle preparation as that shown in A and in Figs 2-9. The shape of the solid line is based on earlier experiments where a wider range of values was obtained (see text):  $P/P_0 = 1 + K_1(\Delta L/L_0) + K_2(e^{-(\Delta L/L_0)/\lambda} - 1)$ , where  $K_1$ ,  $K_2$  and  $\lambda$  are constants. The values,  $K_1=21$ ,  $K_2=0.0048$  and  $\lambda=0.015$ , were chosen to give a good match between predicted and observed force during stimulation (see Fig. 8 and text). The open circles show results for nine other dogfish muscle preparations. (D) The relationship between force during a ramp movement and the velocity of movement (see text). Different symbols are for different muscle preparations. The open symbols are results from Curtin and Woledge (1988). Force  $P$  is expressed relative to the isometric force before movement, and velocity  $V_{CC}$  is expressed as multiples of  $L_0 s^{-1}$ . The red line is based on these observations and matching the predicted and observed force during stimulation (see Fig. 8 and text). At  $P < 0.798$ ,  $V_{CC} = V_{max}(1 - Pm)/(1 + Pmg)$ , where  $V_{max} = 3.8 L_0 s^{-1}$  (Curtin and Woledge, 1988),  $g = 3.7$  and  $m = 0.8$ . This is a rearrangement of Hill's hyperbola; see Woledge *et al.* (1985, p.49).  $m$  is 1/intercept on the force axis and  $g$  is the constant determining the curvature of the hyperbola. The dotted line is the continuation of the hyperbolic relationship shown for  $P < 0.798$ . At  $P > 1.02447$ ,  $V_{CC} = C - [B/(A - P)]$ , where  $A = 1.81$ ,  $B = 0.09$  and  $C = 0.05$ . At  $0.798 < P < 1.02447$ ,  $V_{CC} = q(1 - e^{-(1-P)/f})$ , where  $q = 1.05$  and  $f = 0.41$  (see Edman *et al.* 1976).

## Results

### Experimental results and defining the model

#### Fully active muscle

The characteristics of the series elastic component (SEC) were determined from the results of step-and-ramp shortening experiments. Three sets of superimposed records are shown in Fig. 1A. Fig. 1B shows schematic diagrams of the

corresponding length changes in the whole muscle and its two parts, the SEC and the contractile component (CC). It is important to realise that the force in the SEC is equal to the force in the CC, because these two structures are acting in series. It should also be noted that, although the SEC is shown in the diagram as a single element, in reality it resides in a number of structures as described above. During part a of Fig. 1B, the muscle was stimulated at fixed total muscle length (i.e. SEC plus CC) for 192 ms during which force develops. As the diagram in Fig. 1B shows, the SEC is stretched during this period as the CC develops force and shortens. Then, at b as stimulation continued, the muscle length was rapidly decreased (step) and force declined. During this phase, most of the shortening is taken up by the SEC which can shorten very rapidly, whereas the CC, which relies on much slower crossbridge cycling, shortens only a little. During part c, the muscle shortens at a constant velocity. After the first several tens of milliseconds, the force stabilises. While force is constant, the length of the SEC is also constant and all of the muscle movement is due to CC shortening (sliding of the filaments).

#### *Compliance of the series elastic component*

The relationship between stress and strain in the SEC was found by measuring the size of the length step ( $\Delta L$ ) in Fig. 1A, and measuring the corresponding force,  $P$ . The filled circles in Fig. 1C show the results from a set of four such observations on this muscle preparation. The linear fit (dotted line) through the points for this muscle preparation has a slope of 21 dimensionless units. The stiffness of the SEC is constant over the range of forces we tested for this muscle preparation, as shown by the data points lying close to this line. However, other studies of isolated frog muscle (Jewell and Wilkie, 1958; Hill, 1970), where a wider range of forces were tested, show that the SEC is less stiff at forces below approximately  $0.5P_0$ . This is consistent with observations made in other experiments on dogfish muscle preparations (open circles in Fig. 1C). The solid line is probably a more realistic description of the SEC than is the straight line and is therefore used in later calculations.

#### *The relationship between force and the speed of filament sliding*

In addition to giving information about the SEC, the results shown in Fig. 1A also give information about the relationship between force and the speed of filament sliding ( $V_{CC}$ ) of fully active muscle. As explained above, when force is constant during part c of Fig. 1B, the length of the SEC is not changing, so the velocity of filament sliding ( $V_{CC}$ ) is equal to the velocity of the external movement ( $V_E$ ). Fig. 1D shows data points for force and the velocity of filament sliding for both shortening and lengthening of white fibres from dogfish. Force is expressed relative to the isometric force ( $P_0$ ) just before the step.

In fact, as can be seen in Fig. 1A, force is still increasing at a low rate just before the step change in length; measurements from longer tetani show that at this time it is approximately

93% of the maximum force that can be attained. If releases were to be given at later times, we would expect that the force both during and just before shortening would be a few per cent greater, but their ratio would be the same.

The dotted line in Fig. 1D is a hyperbolic relationship as described by Hill (1938). The solid (red) line shows the relationship we have used. It deviates from Hill's (1938) curve at slow shortening velocities as originally shown by Edman *et al.* (1976). The exact shape of the curve we used was chosen to give both an adequate description of the results in Fig. 1D and also a good prediction of the time course of force, as explained below (see also Fig. 8).

#### *Effects of series elastic compliance on force development*

We have also considered the relationship between force and velocity for two cases where the velocity of filament sliding ( $V_{CC}$ ) differs markedly from the velocity of length change ( $V_E$ ) of the muscle (CC+SEC). In the first case, movement<sub>E</sub> occurs from the *start* of stimulation as crossbridge activity is increasing rapidly (Fig. 2A). In the second case, sinusoidal movement is imposed, with brief periods of stimulation at different phases of the movement<sub>E</sub> cycle (Fig. 2B). In these, we were able to use the measured stiffness ( $S$ ) of the SEC (Fig. 1C) to infer the rate of filament sliding, shown as the bottom graph in each panel of Fig. 2, using the equation:

$$V_{CC} = V_E + (1/S)dP/dt, \quad (1)$$

where  $V_{CC}$  is the rate of shortening or lengthening of the contractile component,  $V_E$  that of the overall muscle, and  $dP/dt$  is the rate of change of measured force calculated from the difference in force between the measurement immediately before and after each point in the computation, with a sampling interval of 5 ms. As an example, Fig. 3 shows one set of records made during sinusoidal movement with a stimulus phase of 20%. Fig. 3A shows the observed force, Fig. 3B shows the overall length change (CC+SEC) and the length change of the contractile component, Fig. 3C shows  $V_E$ , which is the overall velocity of movement of CC+SEC and  $V_{CC}$ , the velocity of filament sliding.

From the parallel plots of force and  $V_{CC}$  (Fig. 2), it is possible to construct the dynamic force-velocity curves (force *versus*  $V_{CC}$ ) for tetani during both ramp and sinusoidal movements (Fig. 4). These curves differ from each other and lie generally to the left of the force-velocity curve for fully activated muscle. These discrepancies are likely to be due to the fact that the tetani (Fig. 2) are brief. Thus, the activation is not constant and for much of the time is well below the activation level prevailing during shortening shown in Fig. 1.

Marsh and Olson (1994) compare the dynamic force-velocity curve for scallop adductor muscle during a twitch and sinusoidal movement with that for afterloaded shortening during tetanic stimulation. The detailed shape of their dynamic curve is rather different from that shown here. This probably reflects the difference between the response of dogfish muscle to a brief tetanus and of scallop muscle to twitch stimulation, and also differences in the importance of

the SEC. However, qualitatively, the results are similar in that the dynamic force-velocity relationship for incompletely active muscle lies to the left (lower force at each velocity of shortening) of the relationship for fully active muscle.

*Time course of crossbridge activation*

To determine whether the discrepancies between the different curves in Fig. 4 are satisfactorily accounted for by the developing and incomplete activation during the brief tetani,

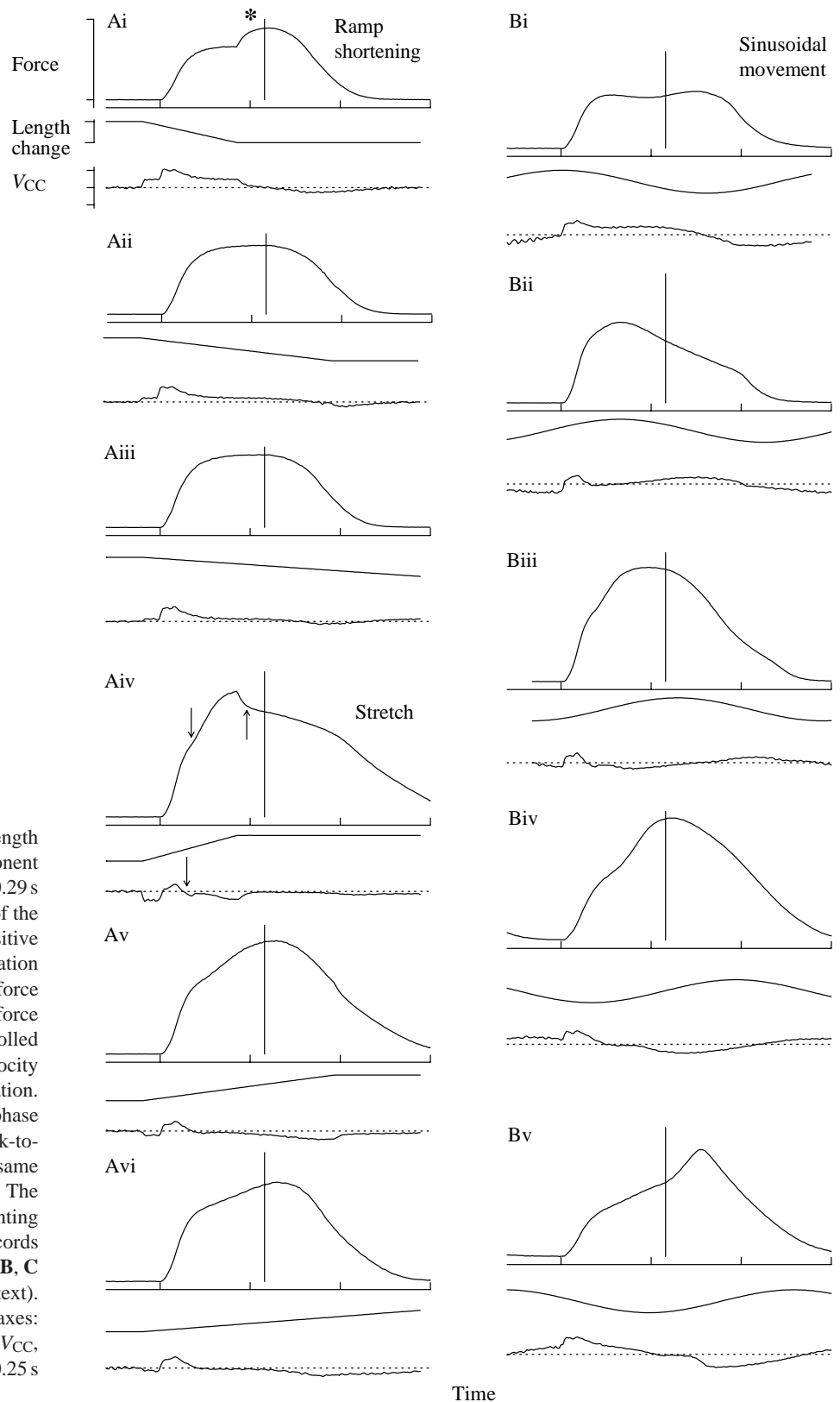


Fig. 2. Records of force and overall length change of the muscle (contractile component plus series elastic component) during a 0.29 s tetanus.  $V_{CC}$  is the velocity of movement of the contractile component (see text). Positive velocity indicates shortening. Stimulation started at the first tick mark below the force record and ended at the vertical line on the force recordings. (A) The motor, which controlled muscle length, moved at constant velocity (ramp) starting 40 ms before stimulation. (B) Sinusoidal movement with different phase relationships to the stimulation. The peak-to-peak amplitude of the movement was the same as the extent of ramp movement in A. The asterisk, downward- and upward-pointing arrows indicate the parts of the records corresponding to the discrepancies labeled B, C and D, respectively, in Fig. 6A (see text). Interval between ticks on the vertical axes: force,  $1.0P_0$ ; length change,  $0.125L_0$ ;  $V_{CC}$ ,  $0.6L_0s^{-1}$ . Horizontal scale is time with 0.25 s between ticks.

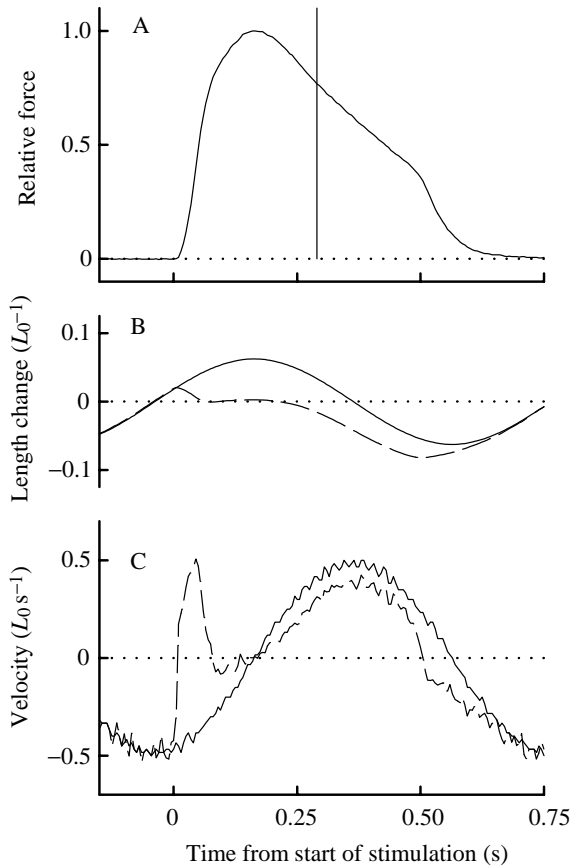


Fig. 3. Force, length change and velocity for imposed sinusoidal movement with a stimulus phase of 20%. The vertical line on the force record marks the end of stimulation. The solid lines for length change and velocity refer to the external movement imposed on the muscle (contractile component plus series elastic component, SEC) by the motor. The broken lines are the length change of the contractile component and the velocity of filament sliding, calculated as described in the text by taking account of the compliance of the SEC. Force is expressed relative to the isometric force  $P_0$ .  $L_0$  is the muscle length at which isometric force is maximal.

we have incorporated a simple model of the dynamics of activation (Fig. 5). A crossbridge activation parameter ( $XA$ ) is expressed relative to full activation (1.0, with the maximum proportion of crossbridges cycling). This is taken to depend on the free concentration ( $a$ ) of an activator according to the equation:

$$XA = a^n / (a^n + K_m^n), \quad (2)$$

where  $K_m$  is the value of  $a$  at which 50% of the crossbridge activation sites are occupied, and  $n$  is the Hill coefficient expressing the cooperativity of binding. The activator concentration ( $a$ ) changes with time and is itself modelled as the concentration in a simple compartment to which activator is added at a constant rate during stimulation and from which it is removed at a rate proportional to  $a$ . Although very simple, this model is not completely unrealistic; it is well

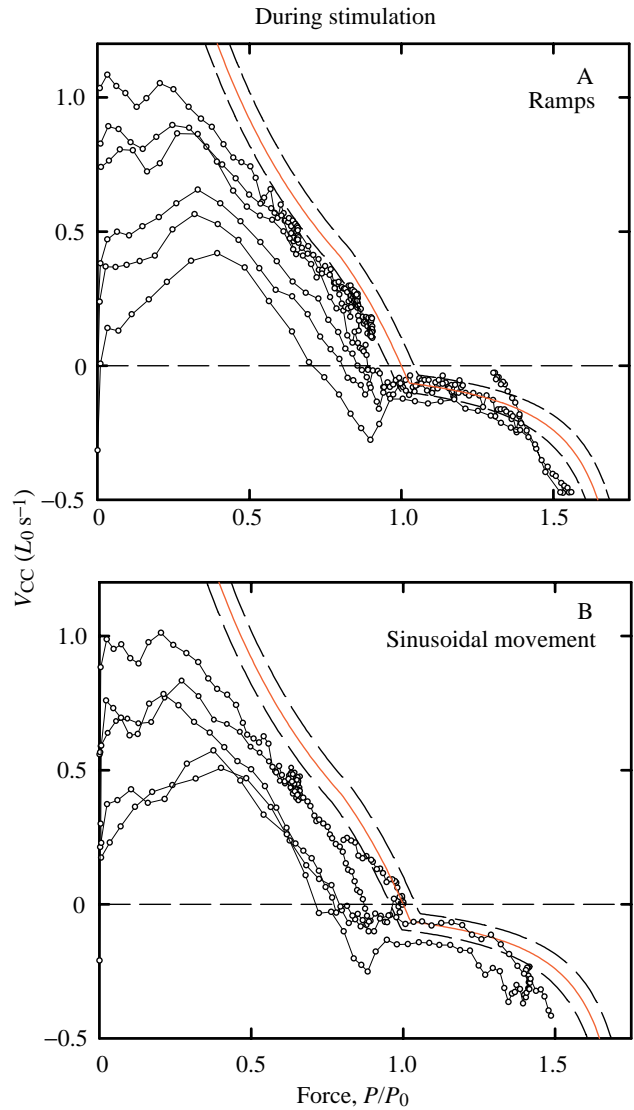


Fig. 4. Relationship between the velocity of movement of the contractile component,  $V_{CC}$ , and force during brief tetani. Points are values recorded at 5 ms intervals with lines joining points for the same tetanus. Note that the low force points are from early in the tetanus when the muscle is not fully active. (A) Results for ramp (constant-velocity) movement. (B) Results for sinusoidal movement and five different phases of stimulation. Fig. 2 shows records of force and  $V_{CC}$  calculated from the records of length and the compliance of the series elastic component as described in the text. The red line is the force-velocity relationship for fully active muscle shown in Fig. 1D. The broken lines are for comparison with Fig. 6 (see Fig. 6 and text).  $L_0$  is the muscle length at which isometric force ( $P_0$ ) is maximum.

known from experiments on 'skinned' fibres, where the concentration of free  $Ca^{2+}$  around the filaments can be controlled, that there is a sigmoidal relationship between isometric force and free  $Ca^{2+}$  concentration (see, for example, Godt and Nosek, 1989).

In our model, the constants are chosen so that  $a$  is relative to the maximum value that it would reach with prolonged

stimulation ( $a=1.0$ ) with an exponential time constant of rise and fall of  $\tau$ .

$$da/dt = (1 - a)/\tau \quad (\text{during stimulation}) \quad (3)$$

$$= -a/\tau \quad (\text{otherwise}). \quad (4)$$

Values of  $K_m$ ,  $n$  and  $\tau$  were chosen that gave a good agreement between the predicted and observed force during stimulation (see Fig. 8). These values were  $n=2.55$  (dimensionless) and  $K_m=0.271$ .  $\tau$  values in the range 0.114–0.150 s were used. The value of  $\tau$  was progressively increased because the rise and fall of force became slower during the experiment. Fig. 5B shows the time course of  $XA$  for the first and last tetani in the series.

#### Velocity of filament sliding and force normalised for crossbridge activity

We will now test the hypothesis that the  $V_{CC}$  depends on the ratio force/ $XA$ , which is a measure of the force exerted per active crossbridge site.

#### During stimulation

Fig. 6 shows the relationship between the velocity of filament sliding and force/ $XA$ . Only points for times *during*

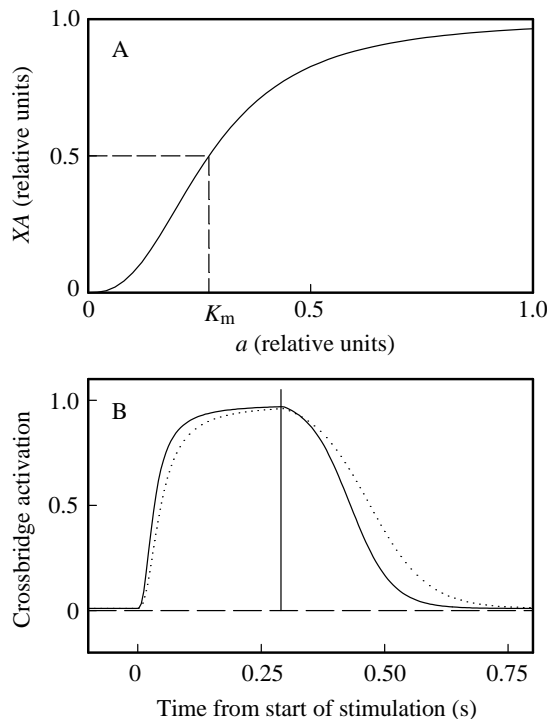


Fig. 5. (A) The assumed relationship between the concentration of free activator,  $a$ , and the extent of crossbridge activation,  $XA$ . At full activation,  $XA=1.0$ . Activator concentration is expressed relative to the final steady concentration of activator that would be reached with sufficiently long stimulation:  $XA=a^n/(a^n+K_m^n)$ , where  $K_m$  ( $=0.271$ ) and  $n$  (2.55) are constants. See text for further details. (B) The time course of crossbridge activation ( $XA$ ) calculated from A for a 0.29 s tetanus assuming values of 0.114 s (solid line) and 0.150 s (broken line) for the time constant ( $\tau$ ) of activator uptake after the end of stimulation (vertical line). See text for further details.

stimulation are shown (relaxation will be considered separately below). Most of the points for the different records do superimpose, in contrast to the results shown in Fig. 4.

The solid (red) lines in Fig. 6 show the relationship between  $V_{CC}$  and force for fully active muscles shown in Fig. 1D, with broken lines showing  $\pm 0.03$  limits for force and velocity. Fig. 6A shows the results for the ramp movements, where each point is calculated from the force values recorded at 5 ms intervals. Most

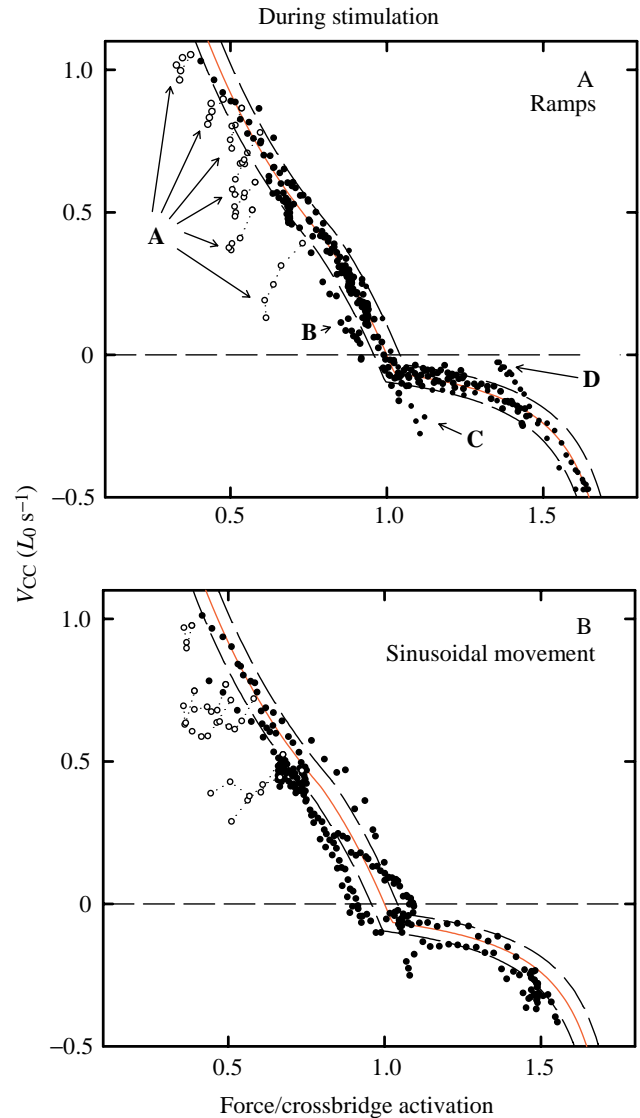


Fig. 6. Relationship between the velocity of movement of the contractile component,  $V_{CC}$ , and the ratio of force to the degree of crossbridge activation during brief tetani. Points are calculated from force values recorded at 5 ms intervals. (A) Results for ramp (constant velocity) movement. (B) Results for sinusoidal movement and five different phases of stimulation. The red line is the force–velocity relationship for fully active muscle shown in Fig. 1D. Most of the points fall within 0.03 force/crossbridge activation units and  $0.03 L_0 s^{-1}$  (broken lines) of the red line. Open symbols (A) are from the first 40 ms after the start of stimulation. B, C and D indicate other discrepancies between the points and the line which are described in the text.  $L_0$  is the muscle length at which isometric force is maximal.

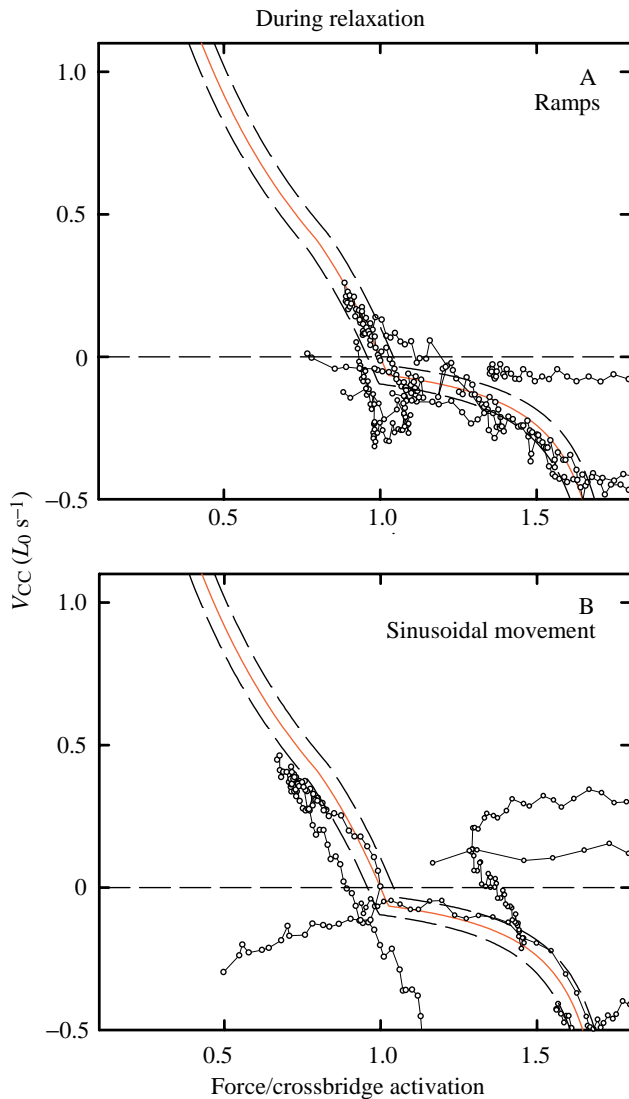


Fig. 7. Relationship between the velocity of movement of the contractile component,  $V_{CC}$ , and the ratio of force to the degree of crossbridge activation during relaxation (after the end of stimulation). Points are calculated from force values recorded at 5 ms intervals, lines join points for the same record. (A) Results for ramp (constant-velocity) movement. (B) Results for sinusoidal movement and five different phases of stimulation. The red line is the force–velocity relationship for fully active muscle shown in Fig. 1D. Most of the points fall beyond 0.03 force/crossbridge activation units and  $0.03 L_0 s^{-1}$  (broken lines) of the red line (see text).  $L_0$  is the muscle length at which isometric force is maximal.

of the points (380/472 or 80.5%) lie within the  $\pm 0.03$  envelope around the line for fully active muscle. We conclude from this good correspondence that the force during movement depends on *both* the velocity of filament sliding and the proportion of the crossbridges that are active and cycling ( $XA$ ).

Some comments can be made about the relatively small proportion of points (19.5% in Fig. 6A) that are outside the  $\pm 0.03$  limits. (1) All points for the first 40 ms of stimulation lie below the curve (these points are shown by the open symbols

in Fig. 6A, labelled **A**). There is a ‘latent period’ of approximately 10–20 ms between the first stimulus and the first rise of force (Abbott and Ritchie, 1951), but this is too brief to explain the discrepancy shown here. (2) The points for the period after the end of the most rapid external shortening (asterisk in Fig. 2Ai) lie below the curve Fig. 6 (labelled **B**). (3) The points labelled **C** in Fig. 6 are from the start of stretch of the contractile component (downward arrow in Fig. 2Aiv) during the contraction with the most rapid external stretch. In Fig. 6A, force/ $XA$  is lower than that observed during stretches at equivalent velocities in other records. (4) The points labelled **D** in Fig. 6A are from the period following cessation of the external stretching (upward arrow in Fig. 2Aiv) during the contraction with the most rapid external stretch. These force/ $XA$  values are higher than expected from the marked decrease in stretching velocity.

The corresponding comparison is made for sinusoidal movement in Fig. 6B. The match is not quite as good as for the ramp movement, but the pattern is similar. Most of the data points (253/413 or 61.3%) are within the envelope around the force–velocity relationship for fully active muscle. Taking account of changing crossbridge activation removes most of the variation seen in Fig. 4. Discrepancies such as 1–3 described above (**A**, **B** and **C** in Fig. 6A) remain.

#### *During relaxation after the end of stimulation*

Fig. 7 shows the relationship between filament sliding velocity and the degree of force/crossbridge activation for times after the end of stimulation. A high proportion of the points during relaxation do not match those during stimulation (compare with Fig. 6). Clearly, additional or different factors are influencing  $V_{CC}$  and/or force during relaxation compared with stimulation.

#### *Calculating force records for comparison with experimental records*

It is now possible to predict the time course of force for each imposed pattern of length change and stimulation using the relationships described above. The resulting predicted time course of force can then be compared with that observed.

The force was calculated in each time step using an iterative method (adaptive Runge–Kutta method implemented in MathCad 6.0) based on its previous value and the changing values of  $XA$  (calculated as described above),  $V_{CC}$  (related to force/ $XA$  according to Fig. 6) and the rate of change of force  $P$  given by:

$$dP/dt = (V_{CC} - V_E)S. \quad (5)$$

Predicted force (broken lines) and observed records of force (solid lines) are shown in Fig. 8A for imposed ramp movements<sub>E</sub> and in Fig. 8B for imposed sinusoidal movements<sub>E</sub>.

#### *During stimulation*

As shown in Fig. 8, there is reasonable agreement between predicted and observed forces *during the period of stimulation*

(the vertical lines mark the end of stimulation). The discrepancy in the force-velocity relationship during the first 40 ms of stimulation that is prominent in Fig. 6A,B is barely detectable when the predicted and observed records are

superimposed in Fig. 8. This probably reflects the fact that these discrepancies only last for a short time. However, the observed force is less than the predicted force when there is considerable shortening during stimulation (Fig. 8Ai,Bi,v).

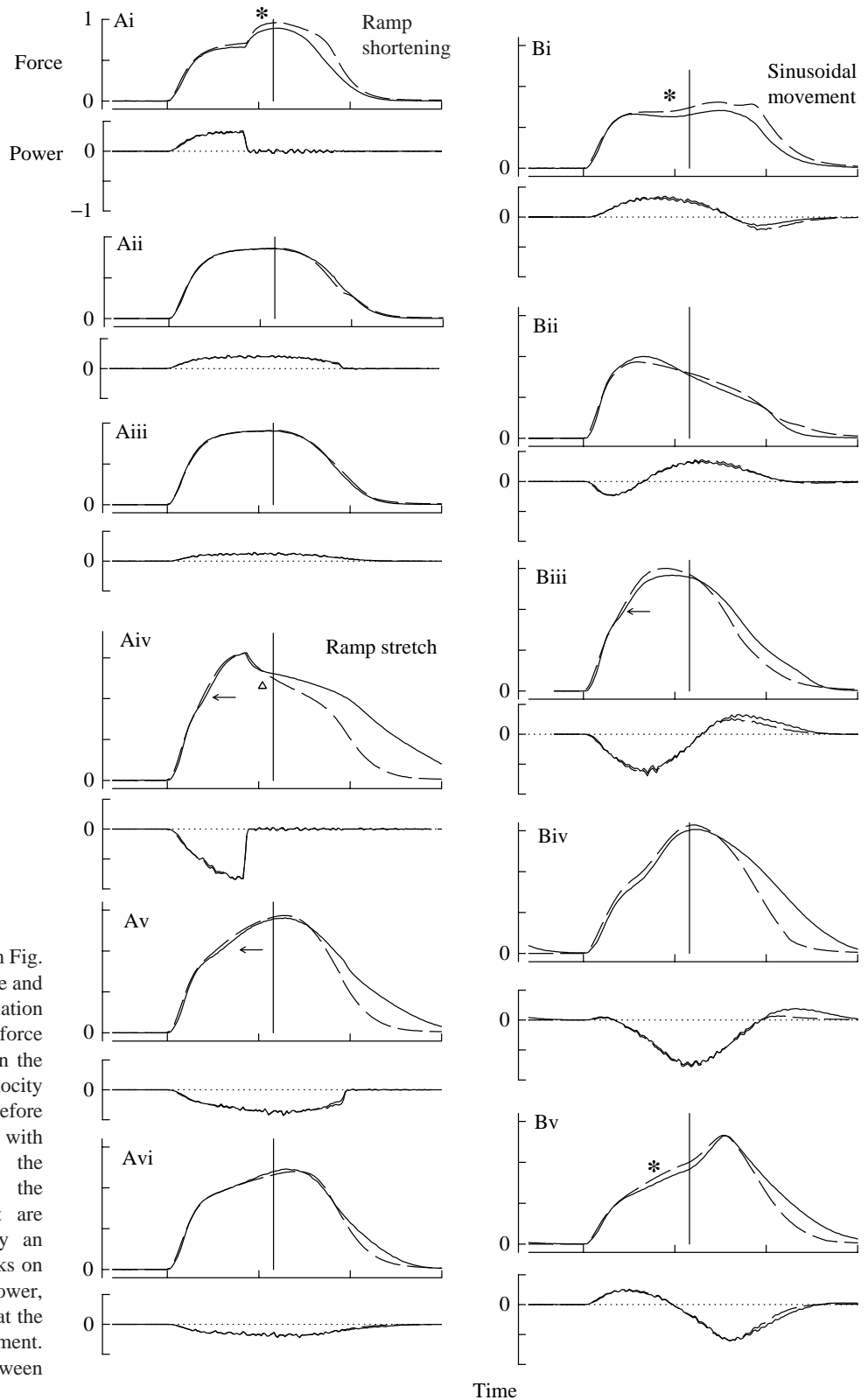


Fig. 8. Records of force (solid lines from Fig. 2) and power and the predictions of force and power (broken lines, see text). Stimulation started at the first tick mark below the force record and ended at the vertical line on the force recordings. (A) Constant-velocity (ramp) movement starting 40 ms before stimulation. (B) Sinusoidal movement with different phase relationships to the stimulation. Discrepancies between the predicted and observed records that are discussed in the text are marked by an asterisk,  $\leftarrow$  and  $\Delta$ . Interval between ticks on the vertical axes: force,  $0.5P_0$ ; power,  $0.5P_0L_0s^{-1}$ . Positive power indicates that the muscle is doing work on the environment. Horizontal scale is time with 0.25 s between ticks.

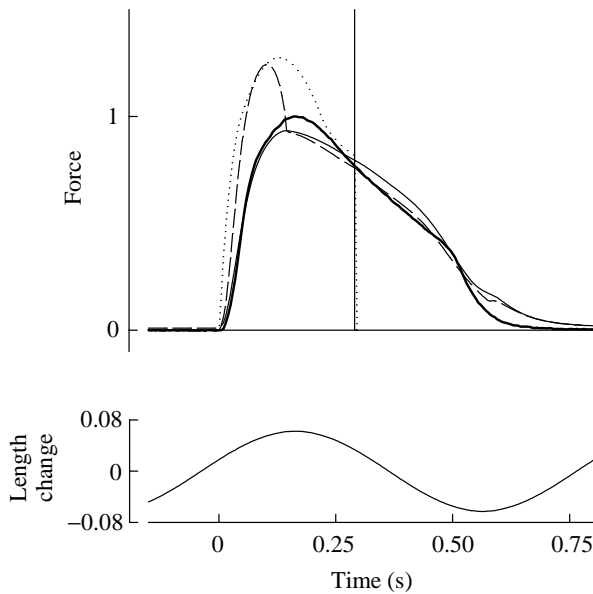


Fig. 9. Time course of force during sinusoidal movement (length change) with stimulation starting at time 0 and ending at 0.29 s (vertical line on the force graph). The bold solid line shows the recorded force, the thin solid line the predicted force (see Figs 2Bii, 8Bii). The broken line shows the predicted force assuming that the series elastic component is infinitely stiff ( $V_{CC}=V_E$ ). The dotted line shows predicted force assuming that the crossbridges are fully active as soon as stimulation starts and that their activation declines to zero as soon as stimulation ends.

#### *During relaxation after the end of stimulation*

The predictions of force during relaxation are generally less good than the predictions of force during stimulation. Predictions for relaxation are best when the muscle was shortening at the end of stimulation (Fig. 8Aii,iii,Bii). The results show that, when the muscle was being stretched at or shortly before the end of stimulation, it produced force for a longer time than predicted (Fig. 8Aiv-vi,Biii-v).

#### *Time course of power output*

Fig. 8 also shows the observations and predictions of instantaneous power output by the muscle (CC+SEC) calculated from observed force and  $V_E$  (motor velocity) and from predicted force and  $V_E$ . The agreement between observed and predicted power is very good. (The small amount of noise on the power curves arises from noise in  $V_E$  and thus affects both the observed and the predicted power.) The discrepancies between the observed and predicted forces during relaxation are less obvious in the power records, because the force discrepancies tended to be greatest when the external movement was zero (Figs 2Ai,iv,v, 8Ai,iv,v) or slow (Fig. 2Bi,iii-v for sinusoidal movement).

### Discussion

Attempts to explain variations of muscle force in terms of SEC elasticity, a force-velocity relationship and a state of

activation have a long history. Well in advance of modern ideas about sliding filaments, Hill (1938) introduced the concepts of the force-velocity curve and the series elastic component, which have stood the test of time and seem to apply to muscle in all its forms. Hill (1938) calculated the time course of rising force at the start of a fixed-end tetanus and during isovelocity shortening, making the important assumption that the 'active state' increased suddenly to its full value at the start of the tetanus. By 'active state', Hill meant the state of the muscle in which energy transduction could occur, as distinct from the resting state in which there was no energy transduction. (The term 'active state' was adopted by other investigators and has acquired various meanings over the years.) Hill considered that the transition between the resting and active states was so fast that it could be treated as instantaneous. He concluded that his predictions of force were generally similar to the observations.

Jewell and Wilkie (1958) made a more quantitative comparison between observed force and that calculated from force-velocity data and the compliance of the series elasticity. They considered only the time course of the rise of force in fixed-end contractions; they assumed full activation, as Hill (1938) did, and used a hyperbolic force-velocity relationship (no deviation at the low shortening velocity end). Jewell and Wilkie (1958) found that the observed time course of the increase in force was slower than the predictions from their calculations, even when the observed redevelopment of force after a release during a fixed-end tetanus was compared with the calculated values.

We have extended the approach used by these authors by taking account of incomplete crossbridge activation ( $XA$ ) during stimulation and relaxation and of the deviation of the force-velocity curve from a hyperbolic relationship at low velocities of shortening. We have applied this approach to patterns of imposed movement not considered in earlier studies; in particular, isovelocity stretch and sinusoidal length changes similar to those likely to occur during *in vivo* locomotion.

#### *Force and $V_{CC}$ during stimulation*

We have found that the time course of force change can be predicted quite well for the period during stimulation provided that due account is taken of the series elasticity that is present and of the time course with which crossbridge activation ( $XA$ ) rises. To illustrate this, Fig. 9 shows predictions in which each of them is omitted. Fig. 9 shows the predicted and observed force for the stimulation pattern (phase 20%) and sinusoidal movement $_E$  used in Figs 2Bii, 8Bii. The broken curve in Fig. 9 was calculated assuming no SEC ( $V_E=V_{CC}$ ), and the dotted curve in Fig. 9 was calculated assuming full crossbridge activation ( $XA=1$ ) from the start of stimulation and return to zero activation immediately at the end of stimulation. In both cases, the predicted force is very different from the observed force and from that obtained using the full model. Thus, each of these factors makes a significant contribution to the shape of the force records.

The good agreement between the predicted and observed

force up to the end of the periods of stimulation in Fig. 8 shows that the principal features of the force and power records during stimulation are reasonably well fitted by taking account of series elasticity and assuming (a) a time course of crossbridge activation that is independent of movement, and (b) a force that is the product of this activation parameter and an invariant force–velocity relationship for the contractile component, independent of the history of the muscle.

#### *Other factors determining force during stimulation*

Although the force and power records during stimulation show good agreement (Fig. 8) and the majority of the points on the corrected force–velocity curves during contraction lie close to the expected curve (force/ $XA$  versus  $V_{CC}$ , Fig. 6), there are some notable discrepancies. These are more obvious in Fig. 6, the plot of force/ $XA$  versus contractile component velocity, which is a more sensitive way of revealing them. These discrepancies, though of interest, are likely to be of less significance in relation to the power production of the muscle (Fig. 8).

*Early times in stimulation.* The sliding velocity of the CC during the first 40 ms of stimulation is considerably lower than would be expected for force and  $XA$  values at that time (open symbols in Fig. 6). It seems that at these *early* times during stimulation there is a different relationship among the determining variables than later or that some additional factor is operating.

*After-effects of shortening.* Edman (1975) and Ekelund and Edman (1982) have described two different mechanisms which produce a depression of force after shortening: ‘shortening deactivation’, which is prominent in twitches and unfused tetani and seems to be due to a reduction in activation by  $Ca^{2+}$ , and ‘force deficit after loaded shortening’, which occurs during tetani and seems to be explained by increased dispersion of sarcomere lengths along the fibre (Edman *et al.* 1993). It seems possible that either or both of these mechanism may explain the discrepancy between our predicted and observed force that is seen when large shortenings of the contractile component have occurred (asterisks in Fig. 8A,B).

*Variations in force during stretch.* The inflections in the records of rising force during stretch ( $\leftarrow$  in Fig. 8A,B) are not predicted by our model. This feature may be related to the well-established fact there is an initial rapid phase of force rise followed by a slower phase when a fully active muscle is stretched at constant velocity (see Woledge *et al.* 1985, pp. 66–71). During the early increase in force, there is increased strain in attached crossbridges (Lombardi and Piazzesi, 1990); this initial increase in force ends when a strain limit is reached. Force subsequently remains high due to rapid reattachment of the bridges forcibly detached by the stretch (Lombardi and Piazzesi, 1990).

*After-effects of stretch.* Our results show that the muscle produces more force after the end of the stretch than the model predicts. This period is indicated by the triangle marking in Fig. 8Aiv (the corresponding clusters of points is marked **D** in Fig. 6). This may represent ‘residual force enhancement after stretch’ which occurs when stimulation continues after the end

of a ramp stretch and more force is produced than would have occurred without the stretch. Evidence from Edman and Tsuchiya (1996) indicates that this ‘residual force enhancement after stretch’ arises as non-uniformity in filament overlap develops along with recruitment of a passive elasticity acting in parallel with weaker regions of the fibre where there is less filament overlap.

It is possible that the matching of predictions to observations might be improved if the factors listed above were taken into account. Clearly, additional experiments would be needed to establish whether each does affect force and, if so, by how much. However, it seems that these factors have rather minor effects on force during stimulation.

#### *Force and velocity during relaxation*

Prediction of force during relaxation is much less successful than are predictions of force during stimulation. We think that this reflects the fact that we have not included in the predictions the internal movements that are known to occur during relaxation (Cleworth and Edman, 1969, 1972; Huxley and Simmons, 1970, 1973; Curtin and Edman, 1989). After the end of stimulation under isometric conditions, force at first declines linearly, then accelerates and becomes approximately exponential. The end of the linear part is called the ‘shoulder’. Curtin and Edman (1989) examined the behaviour along the entire length of muscle fibres by recording the positions of markers placed on the fibres dividing it into several segments. They showed that, at the time of the shoulder, some segments along the length of a muscle fibre start to shorten and stretch others in series with them. The movements of individual segments in relaxation are not just scaled-down versions of the  $V_{CC}$ . The segment movements are more extreme (bigger size and faster than  $V_{CC}$ ), and also the direction may be opposite to that of the overall  $V_{CC}$ . Interventions that delay the shoulder in the force record delay segment movements by the same amount. Cannell (1986) and Caputo *et al.* (1994) have shown that, at the time of the shoulder, the intracellular  $[Ca^{2+}]$  increases, suggesting that the non-uniform length changes at the shoulder enhance the release of  $Ca^{2+}$  from the contractile system.

Thus, it is understandable that the actual time course of force in relaxation is rather different from predictions based on the assumption that the muscle behaves uniformly (with a single value of  $V_{CC}$  at each time). A better match to the force during relaxation might be achieved using a more complex, but more realistic, model in which the contractile component is treated as a series of segments with somewhat different properties.

We thank the Wellcome Trust and the Biotechnology and Biological Sciences Research Council (UK) for financial support.

#### References

- ABBOTT, B. C. AND RITCHIE, J. M. (1951). Early tension relaxation during a muscle twitch. *J. Physiol., Lond.* **113**, 330–335.

- CANNELL, M. B. (1986). Effect of tetanus duration on the free calcium during the relaxation of frog skeletal muscle fibres. *J. Physiol., Lond.* **376**, 203–218.
- CAPUTO, C., EDMAN, K. A. P., LOU, F. AND SUN, Y.-B. (1994). Variation in myoplasmic  $\text{Ca}^{2+}$  concentration during contraction and relaxation studied by the indicator fluo-3 in frog muscle fibres. *J. Physiol., Lond.* **478**, 137–148.
- CLEWORTH, D. AND EDMAN, K. A. P. (1969). Laser diffraction studies on single skeletal muscle fibers. *Science* **163**, 296–298.
- CLEWORTH, D. AND EDMAN, K. A. P. (1972). Changes in the sarcomere length during isometric tension development in frog skeletal muscle. *J. Physiol., Lond.* **227**, 1–17.
- CURTIN, N. A. AND EDMAN, K. A. P. (1989). Effects of fatigue and reduced intracellular pH on segment dynamics in ‘isometric’ relaxation of frog muscle fibres. *J. Physiol., Lond.* **413**, 159–174.
- CURTIN, N. A. AND WOLEDGE, R. C. (1988). Power output and force–velocity relationship of live fibres from white myotomal muscle of the dogfish *Scyliorhinus canicula*. *J. exp. Biol.* **140**, 187–197.
- EDMAN, K. A. P. (1975). Mechanical deactivation induced by active shortening in isolated muscle fibres of the frog. *J. Physiol., Lond.* **246**, 255–275.
- EDMAN, K. A. P., CAPUTO, C. AND LOU, F. (1993). Depression of tetanic force induced by loaded shortening of frog muscle fibres. *J. Physiol., Lond.* **466**, 535–552.
- EDMAN, K. A. P., MULIERI, L. A. AND SCUBON-MULIERI, B. (1976). Non-hyperbolic force–velocity relationship in single muscle fibres. *Acta physiol. scand.* **98**, 143–156.
- EDMAN, K. A. P. AND TSUCHIYA, R. (1996). Strain of passive elements during force enhancement by stretch in frog muscle fibres. *J. Physiol., Lond.* **490**, 191–205.
- EKELUND, M. C. AND EDMAN, K. A. P. (1982). Shortening induced deactivation of skinned fibres of frog and mouse striated muscle. *Acta physiol. scand.* **116**, 189–199.
- FORD, L. E., HUXLEY, A. F. AND SIMMONS, R. M. (1977). Tension responses to sudden length change in stimulated frog muscle fibres near slack length. *J. Physiol., Lond.* **269**, 141–151.
- GODT, R. E. AND NOSEK, T. M. (1989). Changes of intracellular milieu with fatigue or hypoxia depress contraction of skinned rabbit skeletal and cardiac muscle. *J. Physiol., Lond.* **412**, 155–180.
- HILL, A. V. (1938). The heat of shortening and the dynamic constants of muscle. *Proc. R. Soc. Lond. B* **126**, 136–195.
- HILL, A. V. (1970). *First and Last Experiments in Muscle Mechanics*. London: Cambridge University Press.
- HUXLEY, A. F. AND SIMMONS, R. M. (1970). Rapid ‘give’ and the tension ‘shoulder’ in the relaxation of frog muscle fibres. *J. Physiol., Lond.* **210**, 32P–33P.
- HUXLEY, A. F. AND SIMMONS, R. M. (1973). Mechanical transients and the origin of muscle force. *Cold Spring Harbor Symp. quant. Biol.* **37**, 669–680.
- JEWELL, B. R. AND WILKIE, D. R. (1958). An analysis of the mechanical components in frog’s striated muscle. *J. Physiol., Lond.* **143**, 515–540.
- LOMBARDI, V. AND PIAZZESI, G. (1990). The contractile response during steady lengthening of stimulated frog muscle fibres. *J. Physiol., Lond.* **431**, 141–171.
- MARSH, R. L. AND OLSON, J. M. (1994). Power output of scallop adductor muscle during contractions replicating the *in vivo* mechanical cycle. *J. exp. Biol.* **193**, 139–156.
- WILLIAMS, T. L., BOWTELL, G. AND CURTIN, N. A. (1997). Predicting force generation by lamprey muscle stimulated intermittently during imposed length change. *J. Physiol., Lond.* (in press).
- WOLEDGE, R. C., CURTIN, N. A. AND HOMSHER, E. (1985). *Energetic Aspects of Muscle Contraction*. London: Academic Press.